



TITLE:

Improvement in the Power Output of a Reverse Electrodialysis System by the Addition of Poly(sodium 4-styrenesulfonate)

AUTHOR(S):

Yusuke, YAMADA; Keisei, SOWA; Yuki, KITAZUMI; Osamu, SHIRAI

CITATION:

Yusuke, YAMADA ...[et al]. Improvement in the Power Output of a Reverse Electrodialysis System by the Addition of Poly(sodium 4-styrenesulfonate). *Electrochemistry* 2021, 89(5): 467-471

ISSUE DATE:

2021-09-05

URL:

<http://hdl.handle.net/2433/276773>

RIGHT:

© The Author(s) 2021. Published by ECSJ.; This is an open access article distributed under the terms of the Creative Commons Attribution 4.0 License (CC BY), which permits unrestricted reuse of the work in any medium provided the original work is properly cited.



Improvement in the Power Output of a Reverse Electrodialysis System by the Addition of Poly(sodium 4-styrenesulfonate)

Yusuke YAMADA,[§] Keisei SOWA,^{§§} Yuki KITAZUMI,^{§§} and Osamu SHIRAI^{*、§§}

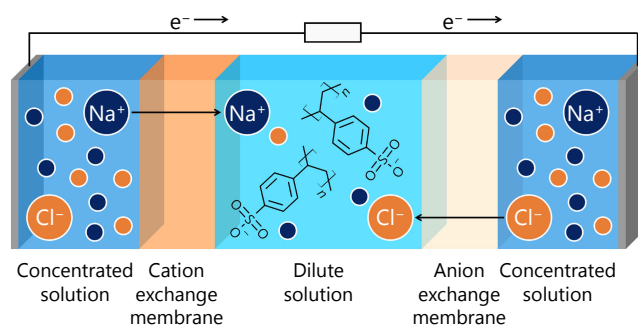
Division of Applied Life Sciences, Graduate School of Agriculture, Kyoto University, Kitashirakawa Oiwake-cho, Sakyo, Kyoto 606-8502, Japan

* Corresponding author: shirai.osamu.3x@kyoto-u.ac.jp

ABSTRACT

Salinity gradient energy generated by the contact between seawater and river water is one of the promising renewable energies. In the reverse electrodialysis (RED), salinity gradient energy is directly translated into the electricity. The representative problem is a large electrical resistance of river water or dilute solutions. The dilute solutions are poor electrically conductive. This results in a huge energy loss when an electrical current passes through it.

In this study, sodium chloride (NaCl) or poly(sodium 4-styrenesulfonate) (NaPSS) was added to the dilute solutions to increase the conductivities and enhance the power outputs of the RED cells. When NaCl was added, the power output reached $11.4 \pm 0.6 \mu\text{W}$. On the other hand, when NaPSS was added, the power output increased up to $19.6 \pm 0.6 \mu\text{W}$.



© The Author(s) 2021. Published by ECSJ. This is an open access article distributed under the terms of the Creative Commons Attribution 4.0 License (CC BY, <http://creativecommons.org/licenses/by/4.0/>), which permits unrestricted reuse of the work in any medium provided the original work is properly cited. [DOI: [10.5796/electrochemistry.21-00073](https://doi.org/10.5796/electrochemistry.21-00073)].



Keywords : Reverse Electrodialysis, Poly(sodium 4-styrenesulfonate), Sodium Chloride, Salinity Gradient Energy

1. Introduction

The practical application and widespread use of renewable energy has become an urgent issue due to the increase in energy demand and the growth in need to reduce carbon emissions.^{1–4} In recent years, salinity gradient energy generated from the difference in salt concentration between seawater and river water has been attracting attention as a new renewable energy.^{4–10} One of the advantages of the salinity gradient energy is that it does not depend on the weather, especially compared to solar energy and wind energy.^{4,8,9} Therefore, it is expected that the salinity gradient can provide stable renewable energy. Reverse electrodialysis (RED) is one of the methods to convert salinity gradient energy into electricity.^{4–11} In the RED system, cation-exchange membranes and anion-exchange membranes are alternately stacked to form compartments of concentrated and dilute solutions. Since cations and anions in the concentrated solutions move in the opposite direction to the dilute solutions at the same time, an electric current is generated.

There are several problems in the practical application such as high cost of the membranes,⁴ selection of the proper electrodes and membranes,^{12–14} deterioration in permeability of the membranes caused by coexisting multivalent ions,^{15–22} clogging and fouling of the system,^{23–26} etc. In particular, the large electrical resistance of the dilute solution compartments is a crucial problem.²⁷ Since dilute solutions contain only a small number of ions, their electrical conductivities are very low. Usually, the compartments of dilute

solutions contribute significantly to the overall internal resistance.^{27–31} Therefore, many research groups have improved the cell systems to reduce the electrical resistance of the compartments of dilute solutions.^{27,29,31–35} The simplest method would be to thin the compartments of dilute solutions, and a lot of attempts have improved the efficiency of the power outputs of the RED systems.^{27,29,35} However, excessive thinning the solution compartments inhibited solution exchange, and the power enhancement reached its limit.^{27,35} Therefore, it should be important to consider other methods for further power enhancement.^{10,31–34}

In this research, the effect of a polyelectrolyte dissolved in the dilute solutions was evaluated. Polyelectrolytes can be retained in the aqueous phase using a dialysis membrane.³⁶ The method requires nothing more than river water and seawater during the steady-state operation. While the addition of polyelectrolytes lowers the solution resistance, it can be considered to have less effect on the membrane potential than NaCl. Therefore, further improvement in the power output can be expected. The effect of the composition of the dilute solutions on the power output of the RED system was evaluated by adjusting the concentration of NaCl or the concentration of poly(sodium 4-styrenesulfonate) (NaPSS), which is a typical polyelectrolyte,^{37,38} in the dilute solutions. It was proved that there is an optimal concentration of NaCl or NaPSS to maximize the power output and that the power output using the cell system in the presence of NaPSS is more than that in the absence of NaPSS.

2. Experimental

2.1 Materials and chemicals

Poly(sodium 4-styrenesulfonate) (NaPSS, $M_w \sim 70000$) was purchased from Sigma-Aldrich Co. LLC. Sodium chloride (NaCl)

[§]ECSJ Student Member

^{§§}ECSJ Active Member

O. Shirai orcid.org/0000-0003-1317-6243

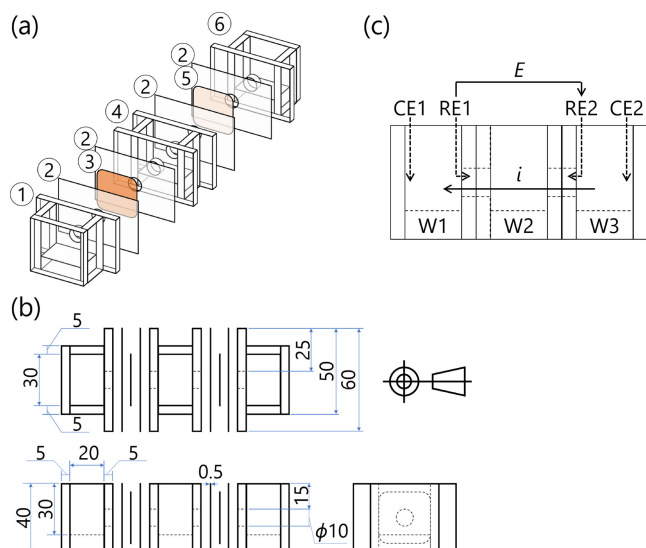


Figure 1. (a) Construction of a RED cell. 1: The concentrated solution phase (W1). 2: 0.5-mm-thick silicone sheets. 3: The monovalent cation-exchange membrane (CIMS). 4: The dilute solution phase (W2). 5: The monovalent anion-exchange membrane (ACS). 6: The concentrated solution phase (W3). (b) The dimensions of the RED cell. The unit of length is millimeter. (c) The arrangement of the electrodes and the definition of the cell potential E and the current i . RE1 and RE2: The reference electrodes (Ag|AgCl|sat. KCl). CE1 and CE2: The counter electrodes (Ag|AgCl).

was obtained from FUJIFILM Wako Pure Chemical Corp. A monovalent cation-exchange membrane (Neosepta CIMS, $1.8 \Omega \text{cm}^2$) and a monovalent anion-exchange membrane (Neosepta ACS, $3.8 \Omega \text{cm}^2$) were obtained from Astom Corp.

All aqueous solutions were prepared with ultrapure water ($>18.2 \text{M}\Omega \text{cm}^{-1}$).

2.2 Preparation of the RED cells

Figure 1 shows the structure and the dimensions of the RED cells which were used to evaluate the power output. The cells were mainly composed of three aqueous phases (W1, W2, and W3), and two ion-exchange membranes (CIMS and ACS). W1 and W3 contained 1.00M NaCl aqueous solutions ($M = \text{mol dm}^{-3}$), which corresponded to the concentrated solutions. As for W2, eleven different solutions (Solution a to Solution k) were used. Their compositions are listed in Table 1. The membrane area and the thickness of CIMS were 0.79cm^2 and 0.15mm , respectively, while those of ACS were 0.79cm^2 and 0.13mm , respectively. In order to see the effect of the dilute solution phase more clearly, we set the distance between the two membranes to 3.1cm , which is relatively large compared to the other studies.^{27,29,35}

The cells were assembled as follows. First, each ion-exchange membrane was immersed in 10.0mM NaCl aqueous solution overnight to reach concentration equilibrium. These ion-exchange membranes were put between the aqueous phases together with silicone sheets and clamped with clips. About 12mL of the solutions were poured into the phases, and each phase was stirred for 30min using a stirrer in order to facilitate the distribution of the ions into the membranes. Then, the cell was left for 30min before electrical measurements so that the measurements were able to be performed under quiescent conditions.

2.3 Electrical measurements

Voltammetric measurements were performed using a potentiostat

Table 1. The compositions of the dilute solutions, the electromotive forces E_{emf} , and the conductivities κ_{D} of the cells.

Solution	$c_{\text{NaCl}}/\text{mM}$	$c_{\text{NaPSS}}/\text{mM}^\dagger$	$E_{\text{emf}}/\text{mV}^{\dagger\dagger}$	$\kappa_{\text{D}}/\text{mS cm}^{-1}$
a	10.0	0	202 ± 3	1.18
b	50.0	0	134 ± 3	5.55
c	70.0	0	118 ± 1	7.61
d	100	0	102 ± 1	10.7
e	140	0	87 ± 2	14.6
f	200	0	71.0 ± 0.9	20.5
g	10.0	40.0	176 ± 2	3.54
h	10.0	90.0	160 ± 1	6.42
i	10.0	190	142 ± 2	12.0
j	10.0	490	112 ± 2	27.3
k	10.0	990	82 ± 7	47.0

[†]The concentration of NaPSS is based on monomer units.

^{††}The errors of the electromotive forces were evaluated from the Student t distribution at a 99% confidential level with samples of size 3.

(HA1010mM1A, Hokuto Denko Co.) and a function generator (HB-305, Hokuto Denko Co.). When the number of the stacked membranes is small, the influence of electrodes tends to appear in the power output.^{6,12} Therefore, in order to eliminate the influence of the electrodes, the measurements were performed using a four-electrode system. Homemade flat-plate Ag|AgCl electrodes and Ag|AgCl|sat. KCl electrodes were used as counter electrodes and reference electrodes, respectively. They were set in W1 and W3 as shown in Fig. 1c. The reference electrodes were placed within 5mm of the surface of the ion-exchange membranes. Unless otherwise noted, the potentials were measured against the reference electrode in W1 (RE1), and the currents due to the flow of cations from W3 to W1 were taken to be positive. Current and potential were recorded using an A/D converter (GL900, Graphtec Co.) During the measurements, the electrical cells were placed in an incubator (IC101W, Yamato Scientific Co.), and the temperature was kept at 298K .

Electrical conductivity measurements were conducted using a four-cell conductivity sensor (300-4C-C, HORIBA, Ltd.) attached to a handheld meter (WQ-330, HORIBA, Ltd.). During the measurements, the solutions were maintained at 298K by a temperature controller (SMU-60C, Sansyo Co., Ltd.).

3. Results and Discussion

3.1 Electric properties of the RED cells

Figure 2 shows a cyclic voltammogram (CV) of the RED cell using 10.0mM NaCl aqueous solution as the dilute solution. The CVs of the cells filled with the other solutions are shown in the supporting information (Figs. S1b to S1k). The shapes of the CVs obeyed Ohm's law. Therefore, potentials of $1/2$ times the electromotive forces were applied at $t = 0.0 \text{s}$ between the two reference electrodes (RE1 and RE2) to evaluate the maximum power outputs. Chronoamperograms are shown in Fig. 3 and Figs. S2b to S2k of the Supporting Information. Except for the just after time the potentials were applied, the values of the currents were kept or gradually decreased.

3.2 Comparison of the power outputs

The power outputs P were calculated by multiplying the applied potentials and the observed currents ($P = -iE$). The results are shown in Figs. 4 and S3. In the case of the cells containing only

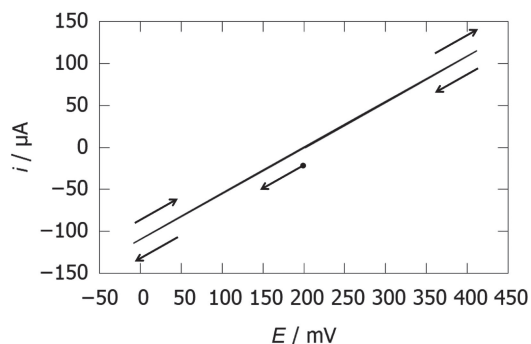


Figure 2. Cyclic voltammogram of the RED cell using 10.0 mM NaCl aq. as the dilute solution. The potential scanning rate: 10 mV s^{-1} .

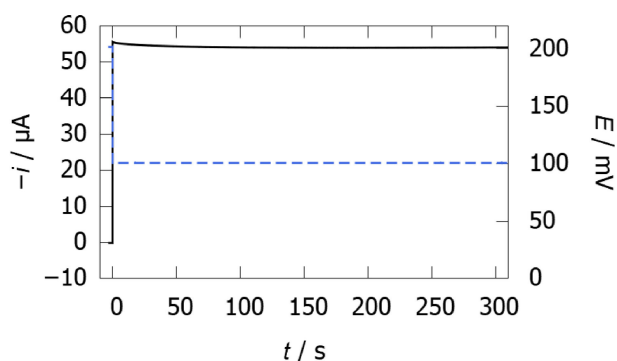


Figure 3. The time-courses of the current i (a solid line) and the applied potential difference E (a dashed line) for the RED cell using 10.0 mM NaCl aq. as the dilute solution.

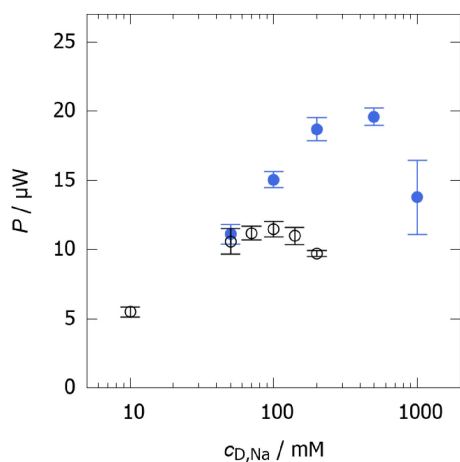


Figure 4. Comparison of the powers P at $t = 300.0 \text{ s}$ against the concentrations of sodium ion in the dilute solutions $c_{D,\text{Na}}$. The error bars were evaluated from the Student t distribution at a 99% confidential level with samples of size 3. (○) and (●) indicate the powers of the cells in the absence and presence of NaPSS, respectively.

NaCl as the electrolytes, the power was the largest when 100 mM NaCl aqueous solution was used as the dilute solution ($P = 11.4 \pm 0.6 \mu\text{W}$). The dependence of the power output on the concentration ratio has been already investigated by several research groups.^{39–41} It has been reported that the power outputs increase

with an increase in the concentrations of both the concentrated and dilute solutions under the condition at the constant concentration ratios. When the concentration of the concentrated solutions is constant, there is an optimal concentration of the dilute solutions which maximizes the power output. The concentration of dilute solutions can be increased by mixing them with concentrated solutions. In addition, since seawater is usually more abundant than river water, it is unlikely that there will be resource constraints. Therefore, it should be useful to mix river water with seawater in an optimal ratio in advance.

On the other hand, when NaPSS was added as an additional electrolyte, the largest power output was obtained when the total concentration of Na^+ was 500 mM ($P = 19.6 \pm 0.6 \mu\text{W}$). The largest value was almost twice as large as that of the cell with the solutions containing only NaCl.

The following model is introduced to explain the results. In this measurement system, the dilute solution phase is much thicker than the other solution phases, and the electrical resistance of the entire cell R_{cell} is considered to be dominated by the electrical resistance of the dilute solution phase. Therefore, we assume that R_{cell} is inversely proportional to the electrical conductivity of the dilute solution as represented by Eq. (1):

$$R_{\text{cell}} = \frac{K}{\kappa_{\text{D}}} \quad (1)$$

where K is the cell constant of the dilute solution phase and κ_{D} is the conductivity of the dilute solutions. It can be thought that the electromotive force E_{emf} is the sum of the membrane potential of CIMS and that of ACS. Since the membrane potential can be represented by the Nernst equation for Na^+ or Cl^- , E_{emf} can be expressed as Eq. (2):

$$E_{\text{emf}} = \frac{RT}{F} \ln\left(\frac{c_{\text{C,Na}}}{c_{\text{D,Na}}}\right) + \frac{RT}{F} \ln\left(\frac{c_{\text{C,Cl}}}{c_{\text{D,Cl}}}\right) = \frac{RT}{F} \ln\left(\frac{c_{\text{C,Na}}c_{\text{C,Cl}}}{c_{\text{D,Na}}c_{\text{D,Cl}}}\right) \quad (2)$$

where R is the gas constant, T is the absolute temperature, F is the Faraday constant, $c_{\text{C,Na}}$ and $c_{\text{C,Cl}}$ are the concentrations of Na^+ and Cl^- in the concentrated solutions, and $c_{\text{D,Na}}$ and $c_{\text{D,Cl}}$ are the concentrations of them in the dilute solutions. The maximum power P_{max} is then represented by Eq. (3) when the potential-current curve obeys Ohm's law.

$$P_{\text{max}} = \frac{E_{\text{emf}}^2}{4R_{\text{cell}}} = \frac{R^2 T^2}{4F^2} \left[\ln\left(\frac{c_{\text{C,Na}}c_{\text{C,Cl}}}{c_{\text{D,Na}}c_{\text{D,Cl}}}\right) \right]^2 \frac{\kappa_{\text{D}}}{K} \quad (3)$$

When the dilute solutions only contain NaCl, $c_{\text{D,Na}} = c_{\text{D,Cl}}$ and $\kappa_{\text{D}} = \Lambda_{\text{NaCl}}c_{\text{D,Na}}$, where Λ_{NaCl} is the molar conductivity of NaCl. Therefore, in this case, the maximum power P_{max} can be expressed as Eq. (4):

$$P_{\text{max}} \propto \left[2 \ln\left(\frac{c_{\text{C,NaCl}}}{c_{\text{D,Na}}}\right) \right]^2 \Lambda_{\text{NaCl}}c_{\text{D,Na}} \quad (4)$$

where $c_{\text{C,NaCl}}$ is the concentration of NaCl in the concentrated solutions.

When the dilute solution contains enough NaPSS and the contribution of Cl^- to the conductivity is negligible, the maximum power P_{max} can be written by Eq. (5):

$$P_{\text{max}} \propto \left[\ln\left(\frac{c_{\text{C,NaCl}^2}}{c_{\text{D,Na}}c_{\text{D,Cl}}}\right) \right]^2 \Lambda_{\text{NaPSS}}c_{\text{D,Na}} \quad (5)$$

where Λ_{NaPSS} is the equivalent conductivity of NaPSS.

Equations (4) and (5) imply that the increase in the concentration of NaCl or NaPSS in the dilute solutions results in the decrease in the electromotive force and the increase in the conductivity. Based on the opposite effects on the power output, the optimal concentration that maximizes the power exists. The major difference between the addition of NaCl and that of NaPSS appears in the

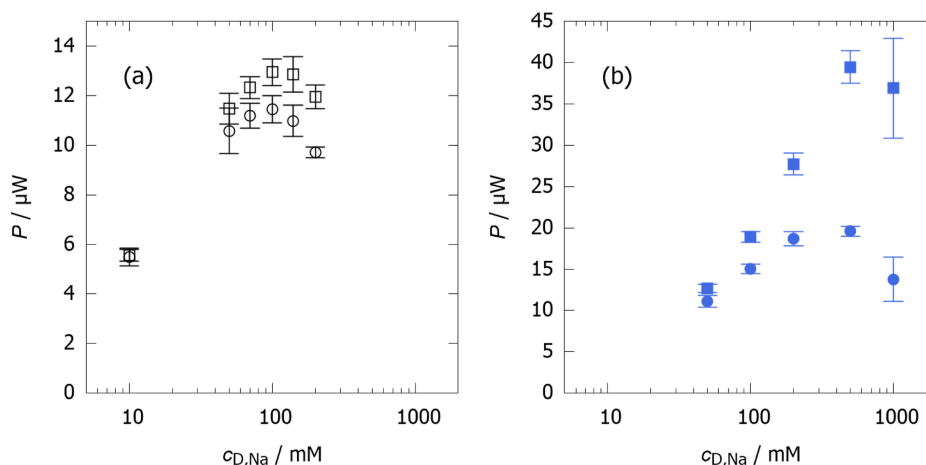


Figure 5. Comparison of the observed power ($t = 300.0$ s) and the calculated power from Eq. (3). The latter was calculated by using the electromotive force and the conductivity in Table 1, together with the cell constant $K = 2.16 \pm 0.03 \text{ cm}^{-1}$. (a) (○) Observed values of the cells in the absence of NaPSS. (□) Calculated values of the cells in the absence of NaPSS. (b) (●) Observed values of the cells in the presence of NaPSS. (■) Calculated values of the cells in the presence of NaPSS.

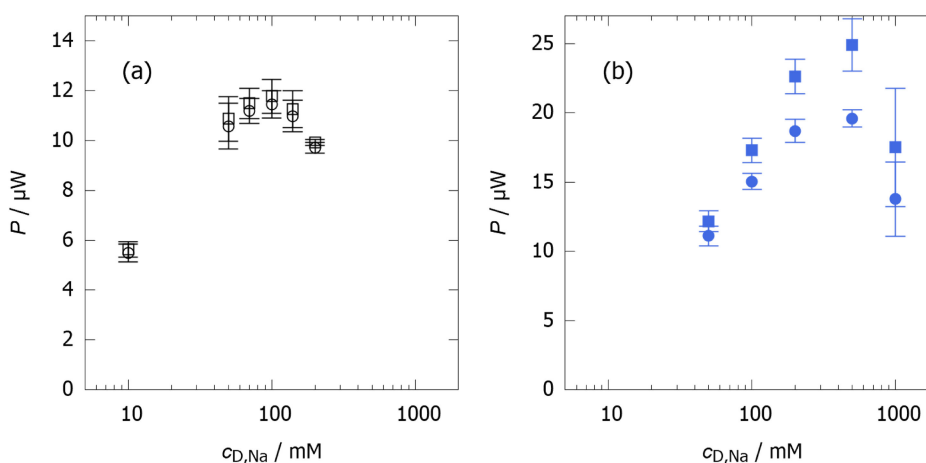


Figure 6. The time-dependences of the powers P . The error bars were evaluated from the Student t distribution at a 99 % confidential level with samples of size 3. (a) (□) P at $t = 0.5$ s of the cells in the absence of NaPSS. (○) P at $t = 300.0$ s of the cells in the absence of NaPSS. (b) (■) P at $t = 0.5$ s of the cells in the presence of NaPSS. (●) P at $t = 300.0$ s of the cells in the presence of NaPSS.

change in the electromotive force. In the case of the addition of NaPSS, the decrease in the electromotive force is reduced because the concentration of Cl^- remains constant. This was confirmed by measuring the membrane potentials E_{mem} (Fig. S4). Therefore, it is considered that the change in the conductivity on the power was dominant even at the higher concentrations, and further improvement of the power was realized.

Figure 5 shows the comparison between the observed powers and the powers calculated from Eq. (3). The cell constant K was calculated from the CVs of the cells using 10.0 mM NaCl aqueous solution as the dilute solutions, and K was evaluated at $2.16 \pm 0.03 \text{ cm}^{-1}$. The experimental results of the electromotive forces and the conductivities, which were used in the calculation, are shown in Table 1.

In Fig. 5, the two types of the powers overlap at the low concentrations, while the difference between them becomes larger at the high concentrations. One of the reasons should be caused by the difference in the total cell resistance (R_{cell}). As the concentration of the electrolytes in the dilute solutions increases, the contribution of them to the total resistance becomes smaller. Therefore, it can be considered that the total resistance could no longer be approximated by the resistance of the dilute solutions, and the effect of ionic permeation of the membranes began to appear.

Furthermore, for the cells using NaPSS, the deviations could also be attributed to time-dependent factors. Figure 6 shows the time-dependence of the power outputs. When the dilute solutions only contained NaCl as electrolytes, there was almost no time-dependence in the power outputs. On the other hand, the cells containing NaPSS showed relatively large time-dependence of the power outputs, especially at the high concentrations.

The anion-exchange membranes should be largely responsible for this time dependence. Figure 7 shows the time-courses of the currents when the potential differences across a single membrane were controlled. The measurements were conducted using similar cells, but they consisted of two water phases (a 1.00 M NaCl aqueous solution phase and a dilute solution phase in the presence of NaPSS) and one ion-exchange membrane. Then a Pt wire was used as the counter electrode in the dilute solution phase. 0 mV was applied as E_{mem} and the currents were normalized by those at 300.0 s after the potential application ($i_{300.0}$) in order to see the changes as ratios. The values of $i_{300.0}$ are listed in Table S1. From Fig. 7, it can be seen that the currents through the CIMS were almost constant, but the currents through the ACS decreased. The reasons for this may include the concentration polarization of Cl^- passing through the ACS, and the adsorption of PSS on the ACS.

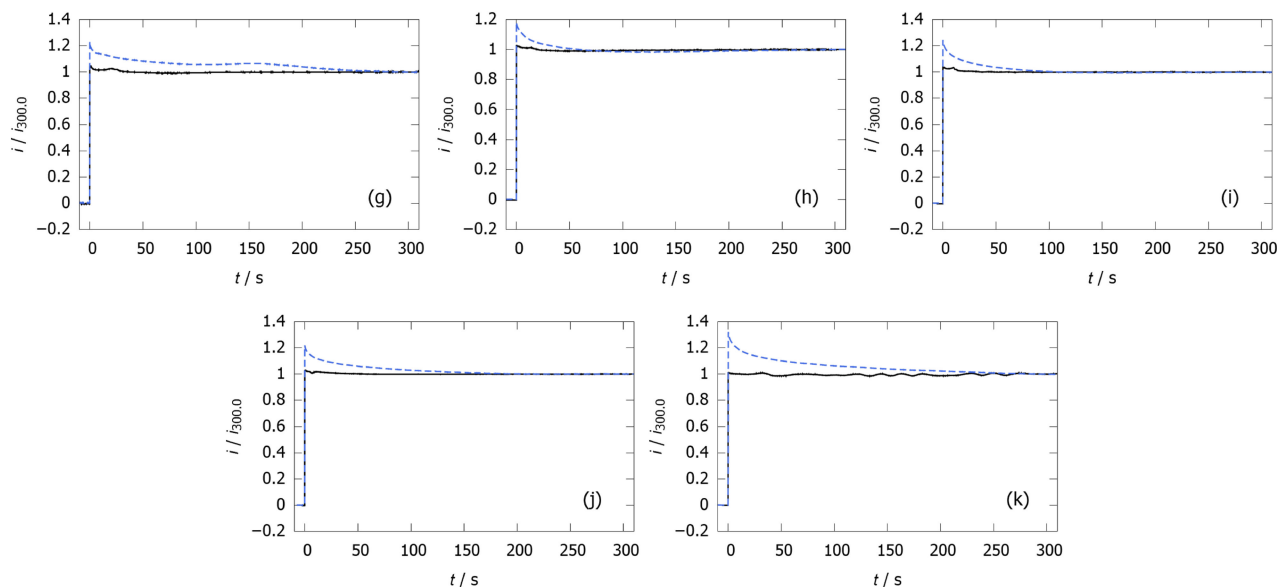


Figure 7. The time-courses of the currents i passing through the CIMS (solid lines) and the ACS (dashed lines) normalized by $i_{300.0}$, the currents at 300.0 s after the potential application. Through the reference electrodes (Ag|AgCl|sat. KCl), 0 mV was applied to the membranes sandwiched between the concentrated solutions (1.00 M NaCl aq.) and the dilute solutions. Ag|AgCl electrodes were used as counter electrodes in the concentrated solutions, while Pt wire electrodes were used in the dilute solutions. The compositions of the dilute solutions: (g) 10.0 mM NaCl, 40.0 mM NaPSS, (h) 10.0 mM NaCl, 90.0 mM NaPSS, (i) 10.0 mM NaCl, 190 mM NaPSS, (j) 10.0 mM NaCl, 490 mM NaPSS, and (k) 10.0 mM NaCl, 990 mM NaPSS.

4. Conclusion

In this study, we investigated the effect of the composition of the dilute solution on the power output. The addition of NaCl increased the conductivity of the dilute solution, but it decreased the electromotive force. The conflicting effect limited the increase in the power output. On the other hand, the addition of NaPSS decreased the solution resistance, but the conflicting effect on the electromotive force was smaller than that of NaCl. Therefore, the power output was about twice as large as that of the NaCl addition.

Data Availability Statement

The data that support the findings of this study are openly available under the terms of the designated Creative Commons License in J-STAGE Data at <https://doi.org/10.50892/data.electrochemistry.15050409>.

References

- P. A. Owusu and S. Asumadu-Sarkodie, *Cogent Eng.*, **3**, 1167990 (2016).
- T. Güneý, *Int. J. Sustain. Dev. World Ecol.*, **26**, 389 (2019).
- F. Sher, O. Curnick, and M. T. Azizan, *Sustainability*, **13**, 2940 (2021).
- A. Zoungrana and M. Çakmakci, *Int. J. Energy Res.*, **45**, 3495 (2021).
- G. Z. Ramon, B. J. Feinberg, and E. M. V. Hoek, *Energy Environ. Sci.*, **4**, 4423 (2011).
- B. E. Logan and M. Elimelech, *Nature*, **488**, 313 (2012).
- Y. Mei and C. Y. Tang, *Desalination*, **425**, 156 (2018).
- R. A. Tufa, S. Pawlowski, J. Veerman, K. Bouzek, E. Fontananova, G. di Profio, S. Velizarov, J. Goulão Crespo, K. Nijmeijer, and E. Curcio, *Appl. Energy*, **225**, 290 (2018).
- J. Jang, Y. Kang, J. H. Han, K. Jang, C. M. Kim, and I. S. Kim, *Desalination*, **491**, 114540 (2020).
- H. Tian, Y. Wang, Y. Pei, and J. C. Crittenden, *Appl. Energy*, **262**, 114482 (2020).
- R. Pattle, *Nature*, **174**, 660 (1954).
- J. Veerman, M. Saakes, S. J. Metz, and G. J. Harmsen, *J. Appl. Electrochem.*, **40**, 1461 (2010).
- O. Scialdone, C. Guarisco, S. Grispio, A. D. Angelo, and A. Galia, *J. Electroanal. Chem.*, **681**, 66 (2012).
- J. G. Hong and J. J. Kim, *New Renew. Energy*, **12**, 53 (2016).
- D. A. Vermaas, J. Veerman, M. Saakes, and K. Nijmeijer, *Energy Environ. Sci.*, **7**, 1434 (2014).
- A. H. Avci, P. Sarkar, R. A. Tufa, D. Messina, P. Argurio, E. Fontananova, G. Di Profio, and E. Curcio, *J. Membr. Sci.*, **520**, 499 (2016).
- A. H. Avci, R. A. Tufa, E. Fontananova, G. Di Profio, and E. Curcio, *Energy*, **165**, 512 (2018).
- J. Moreno, V. Díez, M. Saakes, and K. Nijmeijer, *J. Membr. Sci.*, **550**, 155 (2018).
- L. Gómez-Coma, V. M. Ortiz-Martínez, J. Carmona, L. Palacio, P. Prádanos, M. Fallanza, A. Ortiz, R. Ibañez, and I. Ortiz, *J. Membr. Sci.*, **592**, 117385 (2019).
- A. A. Moya, *J. Membr. Sci.*, **598**, 117784 (2020).
- D. Pintossi, C. L. Chen, M. Saakes, K. Nijmeijer, and Z. Borneman, *npj Clean Water*, **3**, 29 (2020).
- S. Mehdizadeh, Y. Kakihana, T. Abo, Q. Yuan, and M. Higa, *Membranes*, **11**, 27 (2021).
- D. A. Vermaas, D. Kunteng, M. Saakes, and K. Nijmeijer, *Water Res.*, **47**, 1289 (2013).
- H. Susanto, M. Fitrianingtyas, A. M. Samsudin, and A. Syakur, *Int. J. Energy Res.*, **41**, 1474 (2017).
- H. Gao, B. Zhang, X. Tong, and Y. Chen, *J. Membr. Sci.*, **567**, 68 (2018).
- T. Rijnaarts, J. Moreno, M. Saakes, W. M. de Vos, and K. Nijmeijer, *Colloids Surf., A*, **560**, 198 (2019).
- D. A. Vermaas, M. Saakes, and K. Nijmeijer, *Environ. Sci. Technol.*, **45**, 7089 (2011).
- J. W. Post, H. V. M. Hamelers, and C. J. N. Buisman, *Environ. Sci. Technol.*, **42**, 5785 (2008).
- P. Długołęcki, A. Gambier, K. Nijmeijer, and M. Wessling, *Environ. Sci. Technol.*, **43**, 6888 (2009).
- J. Veerman, M. Saakes, S. J. Metz, and G. J. Harmsen, *Chem. Eng. J.*, **166**, 256 (2011).
- B. Zhang, H. Gao, and Y. Chen, *Environ. Sci. Technol.*, **49**, 14717 (2015).
- P. Długołęcki, J. Dąbrowska, K. Nijmeijer, and M. Wessling, *J. Membr. Sci.*, **347**, 101 (2010).
- A. M. Lopez, H. Dunsworth, and J. A. Hestekin, *Sep. Purif. Technol.*, **162**, 84 (2016).
- B. Kang, H. J. Kim, and D. K. Kim, *J. Membr. Sci.*, **550**, 286 (2018).
- S. Mehdizadeh, M. Yasukawa, T. Abo, M. Kuno, Y. Noguchi, and M. Higa, *Membranes*, **9**, 73 (2019).
- J. Požar, K. Bohinc, V. Vlachy, and D. Kovačević, *Phys. Chem. Chem. Phys.*, **13**, 15610 (2011).
- M. R. Talingting, U. Voigt, P. Munk, and S. E. Webber, *Macromolecules*, **33**, 9612 (2000).
- M. Chen, K. Shafer-Peltier, S. J. Randtke, and E. Peltier, *Chem. Eng. J.*, **344**, 155 (2018).
- X. Zhu, W. He, and B. E. Logan, *J. Membr. Sci.*, **494**, 154 (2015).
- V. M. Ortiz-Martínez, L. Gómez-Coma, C. Tristán, G. Pérez, M. Fallanza, A. Ortiz, R. Ibañez, and I. Ortiz, *Desalination*, **482**, 114389 (2020).
- C. Tristán, M. Fallanza, R. Ibañez, and I. Ortiz, *Desalination*, **496**, 114699 (2020).